Integrating Hybrid Area Detectors for Storage Ring and Free-Electron Laser Applications

Heinz Graafsma, Julian Becker, and Sol M. Gruner

Contents

H. Graafsma (✉)
Deutsches Elektronen-Synchrotron (DESY), Center for Free-Electron Laser Science CFEL, Hamburg, Germany
e-mail: heinz.graafsma@desy.de

J. Becker • S.M. Gruner
Cornell University, Ithaca, NY, USA
e-mail: julian.becker@cornell.edu; smg26@cornell.edu

E.J. Jaeschke et al. (eds.), *Synchrotron Light Sources and Free-Electron Lasers*,
DOI 10.1007/978-3-319-14394-1_37

Abstract

Hybrid pixel array detectors (HPADs) have a major impact on the science performed at x-ray synchrotron radiation sources. Broadly speaking, HPADs are of either the photon-counting or integrating variety. The success of photon-counting HPADs at storage rings is well described in the contribution by Brönnimann and Trüb. However, for experiments at x-ray free-electron laser (XFEL) sources, as well as for many fast time-resolved measurements at storage ring sources, photon counting is not an option because too many x-ray photons arrive too quickly for counting electronics to keep up with the local count rate. In these cases, fast analog-integrating systems are mandatory. By using innovative and adaptive front ends, one can achieve both a high dynamic range and a noise sufficiently low for reliable single photon detection. For frame rates above a few tens of kilohertz, temporary in-ASIC frame storage is mandatory. This can be done either in digital or in analog form, each having advantages and disadvantages. HPADs also need to be designed to cope with x-ray damage from extremely high radiation doses provided by current and next-generation x-ray sources. All these developments are summarized, along with some representative groundbreaking experiments performed with integrating HPADs.

Keywords

Hybrid pixel array detector • Integrating x-ray detector • PAD • Xfel

Glossary

AGIPD The **Adaptive Gain Integrating Pixel Detector** (AGIPD) is a dedicated integrating HPAD currently under development for the Eu-XFEL

ASIC An **Application-Specific Integrated Circuit** (ASIC) is an integrated circuit, or micro-electronics chip, customized for a particular use, rather than intended for general-purpose use

CCD **Charge Coupled Devices** (CCDs) have been used as x-ray detectors since many decades and still play an important role in certain applications

CDS **Correlated Double Sampling** (CDS) is a technique to remove undesired offsets and low-frequency noise from a measurement

CMOS **Complementary Metal Oxide Semiconductor** (CMOS) is a technology for constructing integrated circuits

CS-PAD The **Cornell-SLAC Pixel Array Detector** (CS-PAD) is a dedicated integrating HPAD that was developed for use at the LCLS

DEPFET The DEPFET is a **DEpleted P-channel Field Effect Transistor formed in a fully depleted substrate** and acts as a sensor, amplifier, and memory node at the same time

DQE The **Detective Quantum Efficiency** (DQE) is a measure of the combined effects of the signal (related to image contrast) and noise performance of an imaging system

DSSC The **DEPFET Sensor with Signal Compression** (DSSC) is a dedicated integrating HPAD currently under development for the Eu-XFEL

ePix ePix is a **class of x-ray detector architectures** for second-generation LCLS cameras developed by the SLAC detector group

Eu-XFEL The **European XFEL** (Eu-XFEL) is a new x-ray free-electron laser facility currently under construction in the north of Germany

GOTTHARD GOTTHARD (**Gain Optimizing microsTrip sysTem witH Analog ReaDout**) is a 1-dimensional detector system based on the principle of charge integration with automatic gain switching capability

HDR-PAD The **High Dynamic Range PAD** (HDR-PAD) is a successor of the MM-PAD extending its range of applications to experiments at free-electron lasers

HPAD A **Hybrid Pixel Array Detector** (HPAD) consists of two layers of pixelated semiconductors bonded together, pixel-by-pixel, so as to form an imaging x-ray detector unit

JUNGFRAU JUNGFRAU (**adJUstiNg Gain detector FoR the Aramis User station**) is a pixel array detector for high-performance photon science applications at free-electron lasers and synchrotron light sources, currently under development for the SwissFEL

Keck-PAD A pixel array detector designed for microsecond time-resolved x-ray and single bunch imaging

LCLS The **Linac Coherent Light Source** (LCLS) is a free-electron laser facility located at SLAC

LPD The **Large Pixel Detector** (LPD) is a dedicated integrating HPAD currently under development for the Eu-XFEL

MEDIPIX **Medipix** is a family of photon-counting pixel detectors developed by an international collaboration, hosted by CERN

MM-PAD The **Mixed-Mode Pixel Array Detector** (MM-PAD) is designed to have a very wide dynamic range without losing single x-ray sensitivity

MOENCH MOENCH (**Micropixel with enhanced pOsition rEsolution usiNg CHarge integration**) is a hybrid pixel array detector prototype based on charge integration and analog readout, featuring a 25 μm pixel pitch

PSF The **Point Spread Function** (PSF) describes the response of an imaging system to an illumination with a point-like beam

SLAC **SLAC National Accelerator Laboratory**, originally named Stanford Linear Accelerator Center, is a US Department of Energy National Laboratory operated by Stanford University located in Menlo Park, California

SPB The **Single Particles, clusters, and Biomolecules** (SPB) instrument at the Eu-XFEL aims at the investigation of 2D and 3D structures of single particles for scientific investigation in the area of materials sciences, nanomaterials, and structural and cell biology

SwissFEL **SwissFEL** is an x-ray free-electron laser facility currently under construction at the Paul Scherrer Institute in Switzerland

Timepix Timepix is a **detector of the Medipix family** of photon-counting detectors

TSMC The **Taiwan Semiconductor Manufacturing Company** (TSMC) is a semiconductor foundry

XFEL An **x-ray free-electron laser** (XFEL) generates highly coherent intense, short pulses of x-ray light suitable for a variety of scientific research, including chemistry, material science, and studies of macromolecular structure

Introduction

Hybrid pixel array detectors (HPADs), as described in the chapters of this book, have a major impact on the science performed at synchrotron radiation sources. An HPAD consists of two layers of pixelated semiconductors bonded together, pixel-by-pixel, so as to form an imaging x-ray detector unit (Fig. 1). The top *sensor layer*, typically consisting of a silicon chip 0.3–1 mm thick, serves to stop the x-rays and produce free charge carriers, i.e., electrons and holes. Charges are conveyed pixel-by-pixel into an *application-specific integrated circuit (ASIC) layer*. The electronics in each pixel cell in the ASIC processes produces a resultant signal that can be read out and interpreted as the x-ray dose incident onto the pixel.

In this way, numerous desirable characteristics of an imaging x-ray detector are achieved. No single metric characterizes a good detector, and no detector is ideal in all regards (Gruner and Milch 1982; Gruner et al. 2001). However, HPADs excel in a large number of characteristics that are desirable, namely:

1. HPADs have the ability to detect *single x-rays with a high signal-to-noise ratio*. Technically, this is equivalent to saying the detector has a detective quantum efficiency (DQE) near unity in the low flux limit (Gruner and Milch 1982; Gruner et al. 2001).

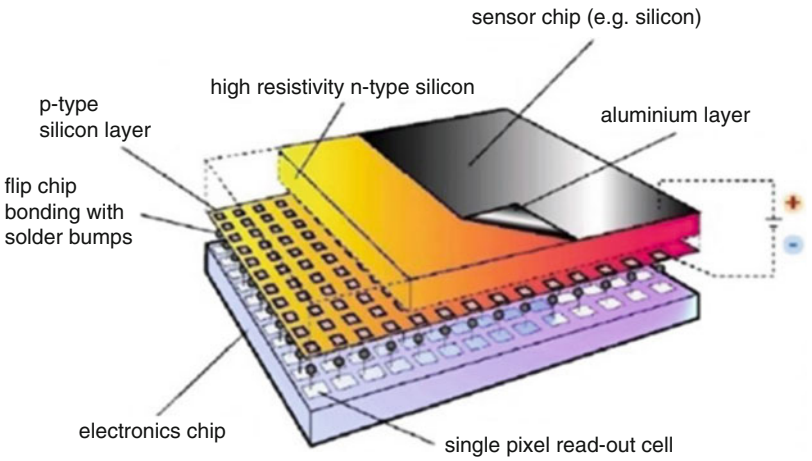

Fig. 1 Typical layout of an HPAD, here showing the Medipix chip in which the sensor layer is bump bonded to an ASIC (Reproduced from MEDIPIX 2014)

2. An ability to capture x-ray signals that range from single photons to many orders of magnitude of x-rays/pixel/s with an accuracy that is dominated by the shot noise in the incident signal, assuming that x-rays arrive randomly over the exposure period. We call this capability *span*. HPADs have excellent span. In this regard, the term *dynamic range* is often used, although technically incorrect.[1] Dynamic range defines the intensity range over which the detector operates, from its noise floor to saturation. But it does not specify that the noise floor is below 1 x-ray/pixel, nor does it demand that the recorded signal be incident signal shot noise limited over this range. The span is ultimately limited by the frame readout rate and the span per image.
3. A point spread function (PSF) (Gruner and Milch 1982; Gruner et al. 2001), both at low and high fluxes, that is essentially one pixel wide. HPADs excel in this regard, especially detectors dependent on phosphor conversion screens fall short.
4. *Stability*. All detectors rely on calibrations that ideally only have to be acquired once. HPADs have excellent stability.

There are other characteristics that may be important for a given experiment, such as the absolute width of the pixel or PSF, x-ray energy discrimination capability, the range of x-ray energies that can be accommodated, cost, ease of use, etc. As stated earlier, no detector is ideal, but HPADs come considerably closer to ideal in many important regards than prior alternative imaging detectors.

Broadly speaking, HPADs divide into two families based on the way the signal is initially processed by the ASIC layer: *Photon counters* discriminate to select pulses corresponding to the arrival of individual x-rays, each of which is then allocated as a count to digital memory, usually within each pixel. Photon counters rely on sequential arrival of x-rays because the signal processing electronics takes finite time (generally 10^{-7}–10^{-8} s) to process a photon count. *Integrators* analog sums the charges arriving at the pixel over some exposure interval, after which this signal is digitized to provide a number proportional to the incident charge, and hence, the total stopped x-ray energy. This is especially important for XFEL experiments, where photon counters would only count up to a single photon per pixel.

For sake of completeness, two other important detector families are briefly mentioned. Firstly, Charge Coupled Devices (CCDs), although commonly not a hybrid system, are a class of integrating detectors which have been widely used for experiments before HPADs became popular and are still unrivaled for certain specialized applications. Secondly, the HPADs are used as vertex detectors in high energy physics. These serve a specialized purpose with their shaping front-end amplifiers and operate like counting detectors but still provide energy information like integrating detectors. This chapter deals specifically with integrating HPADs used in photon science.

Both photon counters and integrators can readily have single x-ray sensitivity and both may be interchangeably used for many – but not all – experiments. An

[1] Despite this, we will use the term dynamic range as a synonym for span in this chapter.

important consideration is that charges produced in the sensor layer typically take tens of nanoseconds to drift to the pixel collection input of the ASIC layer and additional time is needed for the pulse discrimination circuitry to do its work. If many x-rays arrive within this time interval, the charge pulses from individual x-rays pile up on one another and cannot be distinguished. Pulse pileup is readily observed in many experiments because x-rays from storage rings come in <100 ps pulses emanating from circulating charge bunches. Integrators are usually mandatory at XFELs because all the x-rays arrive in ultrashort pulses of <150 fs.

Historical Overview

It was recognized early on that HPADs being developed for high-energy physics applications could make suitable x-ray detectors (Shapiro 1990). The first HPAD, of either the photon-counting or integrating variety to be developed and applied for synchrotron science applications, was the *Cornell "100 × 92" pixel prototype* (Fig. 2). It was an integrator feeding an analog capacitive storage pipeline (Barna et al. 1995; Rossi et al. 1999).

Although this prototype device had many limitations (size, noise, radiation damage susceptibility, etc.), it still served as the enabling detector for previously unfeasible time-resolved studies on shock waves, fuel injectors, and reactive metal foils (MacPhee et al. 2002; Cai et al. 2003; Liu et al. 2004, 2009; Trenkle et al.

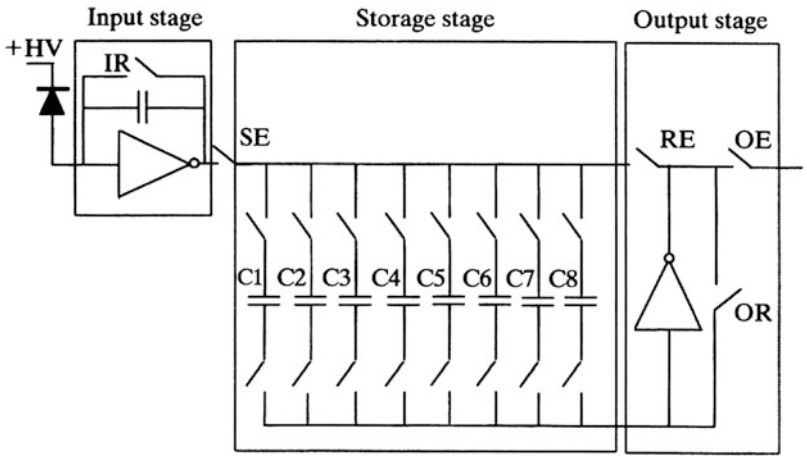

Fig. 2 Pixel schematic of the Cornell 100 × 92 HPAD. Charges stopped in the x-ray sensor pixel diode (left) are charge-to-voltage integrated by the input stage amplifier. The resultant voltage is successively multiplexed onto one of eight storage capacitors by fast transistor switches. The integrator is then reset for a second exposure and multiplexed to a second storage capacitor; this could be done at microsecond rates. After up to eight such successive exposures have been acquired, the input stage is disengaged and all eight stored voltages are analog-to-digital converted and the resultant number is allocated to computer memory (From Rossi et al. 1999)

2008, 2010; Im et al. 2009). In doing so, it helped demonstrate the potential of integrating HPADs to the user community. The 100 × 92 has been replaced by a successor analog pipeline HPAD, called the *Keck-PAD*, which overcomes almost all the key limitations (Koerner et al. 2009b; Koerner and Gruner 2011; Lambert et al. 2014). The Keck-PAD is capable of framing at ∼10 MHz. Versions capable of storing over 30 frames in a multi-tiled format are under development.

When the Linac Coherent Light Source (LCLS), the world's first hard x-ray free-electron laser (at SLAC, the US Department of Energy laboratory near Stanford, California) was approved for construction, it was quickly realized that no existing detector was suitable for general-purpose use at the XFEL. Accordingly, in 2005, collaboration was initiated between Cornell University and SLAC to design, build, and install a suitable integrating HPAD. The Cornell-designed pixel (Fig. 3) utilizes a front end with two selectable gains, the result of which is analog-to-digital converted at the 120 Hz LCLS pulse frequency (Philipp et al. 2007; Koerner et al. 2009a; Philipp et al. 2010, 2011).

The resultant *Cornell-SLAC PAD (CS-PAD)* and its subsequent upgrades (Herrmann et al. 2014, 2013; Hart et al. 2012b) have facilitated an enormous number of scientific breakthroughs and results. A good example is serial x-ray crystallography, whereby a serial stream of protein microcrystals is passed through the LCLS beam and the resultant diffraction data from many randomly oriented microcrystals are

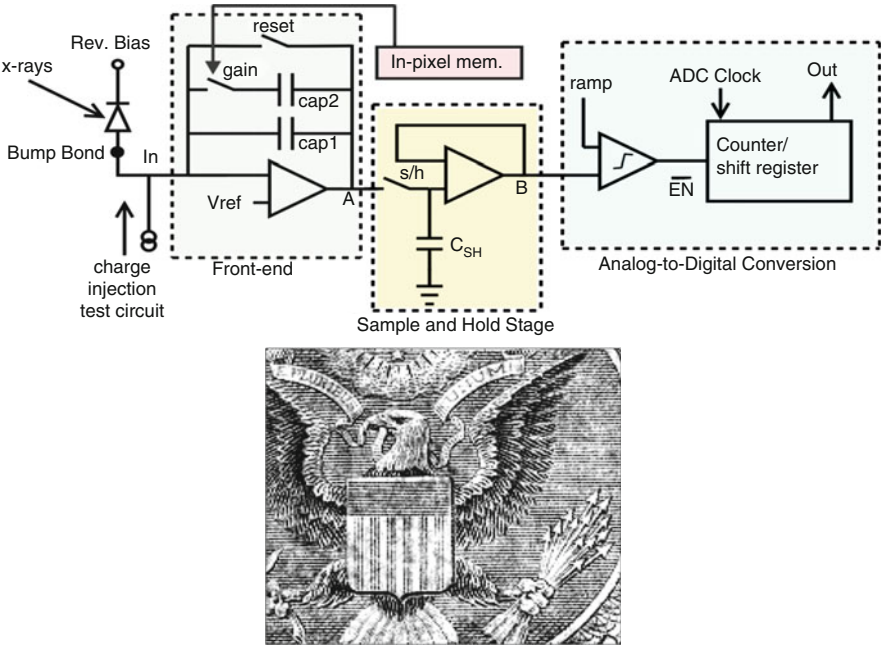

Fig. 3 The Cornell-SLAC PAD (CS-PAD) pixel schematic (*top*) consists of an integrating input stage with two programmable gains. The integrated result is sampled and held and digitized by an in-pixel ADC operating at the LCLS 120 Hz pulse rate. The eagle (*bottom*) is Cu K_α x-radiograph with a detector module of the ink in a section of a US one dollar bill

used to determine the structure of the protein (Boutet et al. 2012). This method has been used, for example, to determine the structures of challenging membrane proteins (Liu et al. 2013) and protein crystals grown in vivo in bacteria (Redecke et al. 2013). SLAC is now developing a second generation of detectors, called ePix, for the LCLS (Dragone et al. 2014).

The integrating HPADs described thus far ultimately store signal as a capacitor voltage that is subsequently digitized. An appropriate combination of well depth and sensitivity is achieved by careful selection of the size of the feedback capacitors engaged by the input amplifier. A very different integrating approach developed by a collaboration of the Cornell group and Area Detector Systems Corporation (Poway, CA, USA) is the *Mixed-Mode PAD (MM-PAD),* as explained in section "Range Extension by Use of a Charge Pump." The MM-PAD both achieves excellent single x-ray sensitivity (Ayyer et al. 2014) and yet spans an enormous dynamic range of $>10^8$ x-rays/pixel/s while framing at >1 kHz; this has proven to be very useful for coherent x-ray imaging (Giewekemeyer et al. 2014). The MM-PAD is designed for use at storage rings and is not suited for XFELs because its charge removal process (see section "Range Extension by Use of a Charge Pump") can be outrun by XFEL pulses. However, the Cornell group is developing a modified version with an even larger dynamic range (HDR-PAD) that would work at both storage rings and XFELs.

Systems and Prototypes Under Development as of Mid-2014

Hard XFEL facilities currently under construction like the European XFEL (Eu-XFEL) and SwissFEL are also catalyzing advances in integrating HPADs. The European XFEL, for example, pushes the envelope for burst mode imaging due to its special timing structure, requiring 4.5 MHz frame rate for 600 us (2,700 pulses) followed by 99.4 ms of idle time.

Again realizing the need for dedicated detector systems for such a demanding experimental environment, a community wide call for Expressions of Interest was launched, ultimately leading to the establishment of three different projects that aim for working systems coinciding with the start of Eu-XFEL operations. These three projects are the Adaptive Gain Integrating Pixel Detector (AGIPD; Henrich et al. 2011; Shi et al. 2010; Becker et al. 2013b; Greiffenberg 2012), the Large Pixel Detector (LPD; Hart et al. 2012a; Koch et al. 2013), and the DEPFET Sensor with Signal Compression (DSSC; Lutz et al. 2010; Fischer et al. 2010; Erdinger et al. 2012). All share common approaches like in-ASIC storage of imaging information, combined with dynamic range extension techniques and sensor thickness of approximately 500 μm.

The *AGIPD* uses a dynamically switched gain stage in the preamplifier (see section "The Adaptive Gain Technique") to reduce the preamplifier gain for large signals on a per-pixel per-frame basis and uses 352 analog storage cell inside the pixel circuitry as random access memory. With $(200\,\mu\text{m})^2$ pixels, the AGIPD has the smallest pixel size of the three Eu-XFEL detectors. Figure 4 shows the 1M-pixel version under construction for the SPB-Station.

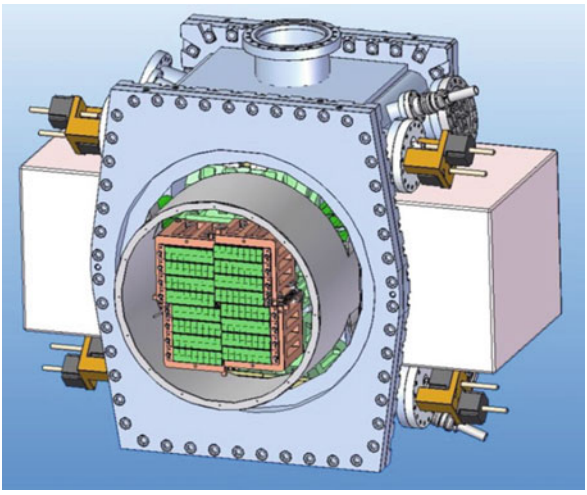

Fig. 4 Layout of the 1M-pixel system under construction for the Eu-XFEL. The sensor arrays (*green, center*) are arranged around a central hole that can be varied in size. The vacuum housing enclosing the heart of the detector is shown

The *LPD* uses three independent gains per pixel in parallel, saving information from all three gain stages in dedicated banks of analog memory which can store 512 images and selects the correct gain stage information to transmit during readout. The pixel size of $(500\,\mu\text{m})^2$ and use of a redistribution layer on the sensor allow a different pitch of pixels and readout nodes. In combination with a clever arrangement of interposer and shielding, this allows abutting modules on all four sides and at the same time partially shielding the ASICs from the radiation.

DSSC on the other hand uses hexagonal pixels of $236 \times 204\,\mu\text{m}^2$, a tailored non-linear gain in either sensor or ASIC, an in-pixel analog to digital converter (ADC), and 640 digital storage cells per pixel. Due to its low noise and optimized entry window, the system can be used down to x-ray energies somewhat below 1 keV.

A detector for SwissFEL application is currently developed by the Swiss Light Source (SLS) detector group at the Paul Scherrer Institute (PSI). This *JUNGFRAU* (adJUstiNg Gain detector FoR the Aramis User station; Mozzanica et al. 2014) system is similar to AGIPD in its 3-stage adaptive gain mechanism and features 16 storage cells within its $(75\,\mu\text{m})^2$ pixels for burst mode exposures. Since the SwissFEL is intended to run at 120 Hz, the detector system can be read out between pulses without the need for extensive in-pixel storage. For synchrotron applications, continuous operation at more than 1 kHz is envisioned.

Another system under development by the PSI group is the *MOENCH* (Micropixel with enhanced pOsition rEsolution usiNg CHarge integration; Dinapoli et al. 2014). MOENCH has promise to redefine the way we think about imaging at low x-ray flux rates. It features extremely small pixels of $(25\,\mu\text{m})^2$, which causes the overwhelming majority of photon detection events to be split between four pixels. While commonly great efforts are made to avoid split events, the low noise of MOENCH allows event reconstruction, and thereby enabling spectroscopic imaging with $<5\,\mu\text{m}$ rms spatial and $<200\,\text{eV}$ energy resolution at frame rate exceeding 6 kHz (Dinapoli et al. 2014).

Sensors for Direct Detection of X-Rays

The sensor in hybrid detectors functions to absorb the impinging x-ray photons and to produce a corresponding electrical signal that is subsequently processed by the readout electronics in the ASIC. When an x-ray photon is absorbed in a solid-state sensor by photo-absorption (the dominant process at the x-ray energies being considered here[2]), its entire energy is deposited within picoseconds, ultimately creating many electron-hole pairs in a small volume roughly a micrometer across. The average energy, ε, required to create one electron-hole pair is related to, but significantly larger than, the bandgap of the material. For example, in silicon, $\varepsilon = 3.6\,\text{eV}$, while the band gap is only 1.1 eV. For germanium, these values are 2.4 and 0.66 eV, respectively. Since the photon deposits its entire energy, E_{ph}, upon absorption, the number of electron-hole pairs created is $n_{\text{eh}} = E_{\text{ph}}/\varepsilon$. The variance, σ_{eh}, in n_{eh} may be smaller than $\sqrt{n_{\text{eh}}}$. This is usually specified by the Fano factor, $F = \sigma_{\text{eh}}^2/n_{\text{eh}}$, which is material dependent; for silicon, $F = 0.1$. Thus, the absorption of a 12 keV x-ray in silicon yields 3333 electron-hole pairs with a variance of 18 electron-hole pairs.

The created electrons and holes drift in opposite directions under the influence of an applied electric field; this constitutes a current that is detected by the readout electronic circuitry. The electric field may be achieved by operating the sensor volume either as a reverse biased diode (i.e., with a depletion region field) or as a photoconductor. Silicon has relatively low resistivity and is usually operated as a reverse biased diode with a nearly fully depleted thickness across the sensor. Other materials, with larger bandgaps, can also be operated as biased photoconductors.

Under room temperature operating conditions, silicon sensors, due to the small bandgap of 1.1 eV, may show significant numbers of thermally generated electron-hole pairs, depending on crystal impurities, as well as temperature-dependent effects of accumulated radiation damage. The resulting "dark" current can be problematic for long integrations. In consequence, integrating HPADs based on silicon sensors often are cooled.

Most HPADs to date utilize silicon sensors 0.3–1 mm thick, with a good resultant stopping power to x-rays of up to roughly 20 keV. A variety of alternative sensor materials, such as Ge, CdTe, CZT, and GaAs, are being investigated for higher x-ray energy applications. GaAs and CdTe, with bandgaps of about 1.4 eV, are attractive beyond their increased stopping power for high-energy x-rays as they can be operated at room temperatures. Dark currents in these materials are commonly dominated by crystal defects and local impurities rather than thermal effects.

The major impediment for alternatives to silicon sensors has invariably been difficulty in obtaining sensor materials of sufficient quality, thicknesses, size, and quantity, as well as difficulties in processing these materials. Nevertheless, progress is being made for all the aforementioned materials.

[2]Typically, this would be the energy range between 1 and 20 keV.

The Application-Specific Integrated Circuit (ASIC)

Development of new detector systems often implies the design of a new application-specific integrated circuit (ASIC) as available ones do not fit the tasks at hand. Although this situation is slowly changing with the increased availability of more universal readout chips like the Medipix and Timepix series developed by CERN (Ballabriga et al. 2013; Poikela et al. 2014), custom designed ASICs are required for a wide range of experiments that simply cannot be performed with "universal" ASICs.

Although the increase in performance and capabilities of new detector generations can in part be attributed to the learning curve of the developing groups, it is also related to the progression to CMOS technologies with smaller feature sizes (Moore's law). A decreased feature size allows more functionality per unit area, but this goes hand in hand with a reduction of the maximum allowed voltage and thus a reduction of the maximum charge that can be stored on a given capacitor. Whereas the 1.2 μm technology used for the 100 × 92 PAD operated at 3.5 V, the 130 nm technology used for AGIPD has a maximum operating voltage of only 1.5 V – less than half of 3.5 V – limiting the usefulness of single gain architectures (see section "Single Gain Architecture") for experiments requiring a large dynamic range. The use of dual voltage processes, allowing lower voltages for the digital and larger voltages for analog parts of the circuity, may be a path forward. Even in this case, available area may still be a concern, as commonly the analog parts cannot be shrunk as much as the digital parts of an ASIC when reducing the feature size.

Integrating Front Ends

As explained in section "Sensors for Direct Detection of X-Rays," the absorbed x-rays create a number of electron-hole pairs proportional to the absorbed energy. Under the influence of an external electric field (bias voltage), charge carriers drift to the readout node, thereby constituting a current. This is conveyed by a connecting bump to the input node of a charge-sensitive integrating amplifier[3] in the readout ASIC pixel (Fig. 2).

In classical charge-to-voltage architectures, the resultant amplifier voltage is directly proportional to the number of electron-hole pairs created and thus to the absorbed x-ray energy. This assumes that no charge carriers are lost during the drift time due to trapping or recombination, which is the case for highly perfect sensor materials like silicon and germanium, and that no charge has leaked away from the integration (feedback) capacitor, which is the case for well-designed amplifiers. The size, C, of this feedback capacitor plays a determining role in the sensitivity as well

[3]Other circuit architectures than dc-coupled charge-sensitive amplifiers are used (e.g., in DEPFET type detectors), but here, we limit ourselves to this architecture, which is the most widely used circuit for HPADs.

as the dynamic range of the amplifier since the voltage, V, across it for a given total integrated charge, Q, is given by the charge-to-voltage conversion ratio, $V = Q/C$.

Integrated circuits generally have total voltage ranges of only a few volts, which seriously constrain the amplifiers that can be practically implemented on an ASIC. Good x-ray sensitivity, i.e., a high charge-to-voltage ratio suggests a small value of C to compete effectively with the amplifier noise voltage. The drawback is that a small capacitor can only store a limited amount of charge before the maximum allowed voltage is reached, thereby limiting the maximum signal that can be recorded. In other words, in the absence of dynamic range extension techniques, one has to find a compromise between having low noise, i.e., a small capacitance and thus high gain, and the ability to handle large signals, i.e., a large capacitance with low gain.

Single Gain Architecture

The 100×92 PAD (Fig. 2) mentioned in the introduction may be used as a numerical example for a single gain integrator. A feedback capacitor of 2 pF was used together with a maximum voltage of 3.5 V, imposed by the 1.2 μm CMOS technology used. This gives a maximum charge ($Q = CV$) that can be stored of 7×10^{-12} C or 4.4×10^7 electrons. With 2,472 electrons generated per absorbed 8.9 keV x-ray, this corresponds to 17,700 x-rays, in agreement with the 17,000 quoted in the paper Rossi et al. (1999). The readout noise of the entire electronic chain was 0.5 mV, which is a typical value, which corresponds to 10^{-15} Coulombs, or 6,240 electrons on a 2 pF capacitor, which is the equivalent signal to 2.5 photons of 8.9 keV absorbed in the silicon sensor. If, on the other hand, one would want to have single photon sensitivity, then the equivalent noise should be less than 1/5th of a photon, a factor 12.5 less. With the readout noise being a constant of approximately 0.5 mV, a single photon has to produce a signal of 2.5 mV on the capacitor, which for 2,472 electrons means a capacitor size of 160 fF. Since the maximum allowed voltage is also a fixed number, this automatically results in a reduction of the maximum signal by the same factor 12.5 giving 1,475 photons.

In order to enlarge the useful operating range of integrating hybrid detectors, the user can sometimes select between two operational modes – high gain, low noise and low gain, high intensity – by switching in or out an additional feedback capacitor. This option was implemented in the CS-PAD system and is schematically given in Fig. 3. Although this increases the usefulness of the system, the user is required to decide beforehand which regions of the detector will be at high gain and which will be at low gain. This requirement of deciding on the gain beforehand can be lifted by implementing charge pumps, automated switching schemes, or using well-defined nonlinear gains, as explained below.

Range Extension by Use of a Charge Pump

One solution to the abovementioned conflict between high sensitivity and large signals is to use a relatively small capacitor for high sensitivity and to remove a well-defined amount of charge from the capacitor each time the voltage over the capacitor reaches a preset threshold. This principle of a charge pump is implemented in the Mixed-Mode PAD (MM-PAD), a collaborative development of the Cornell group

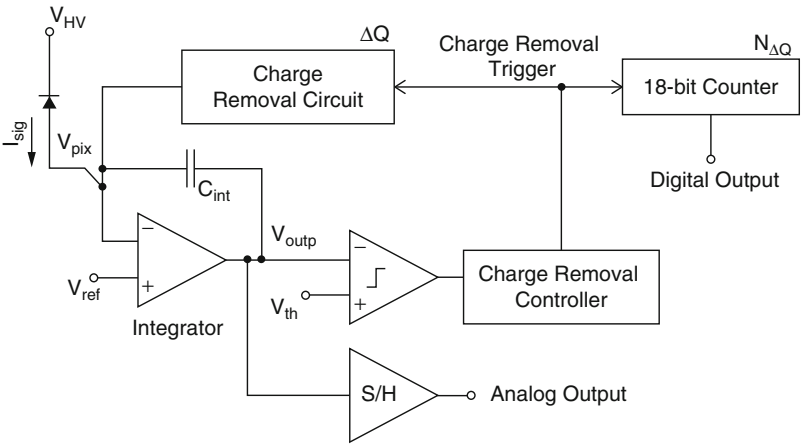

Fig. 5 Schematics of the MM-PAD with a charge removal circuit (charge pump) to achieve a very wide dynamic range

and Area Detector Systems Corporation (Poway, CA, USA), and depicted in Fig. 5 (Vernon et al. 2007; Schuette 2008; Tate et al. 2013).

The ASIC was fabricated using 0.25 μm TSMC technology, with a maximum operating voltage of 2.5 V. For the 50 fF feedback capacitor used, this yields a maximum storage capacity of 7.8×10^5 electrons, which corresponds to roughly 260 photons of 11 keV absorbed in silicon. As charge is being integrated, the resultant integrator voltage is constantly being compared to a threshold voltage, V_{th}. Every time this voltage is crossed, the comparator fires and 80 fC is removed from the feedback capacitor. This threshold is adjustable but is normally set to correspond to the signal generated by 150 x-rays. The charge removal operation occurs simultaneously with arrival of new charge from the sensor, i.e., it incurs no dead time. The number of times charge is removed and is stored in an 18 bit counter inside the pixel. At the end of the exposure time, both the counter and the remaining charge on the feedback capacitor are read out, giving the total charge that has been integrated. With the 18 bit counter, a total signal of $2^{18} \times 150 = 4 \times 10^7$ photons of 11 keV can be recorded. The measured readout noise of the detector is 350 electrons equivalent (= 1.1 mV over 50 fF) corresponding to 0.11 photons of 11 keV. Therefore, for short exposure times, also single photon sensitivity is achieved. For longer exposure times, the integrated dark current will eventually limit the sensitivity, so the device is commonly cooled to reduce dark current. At the normal MM-PAD operating temperature of −30 °C 240 s are required for the dark current noise to be equivalent to an x-ray (Tate et al. 2013). For signals below the threshold limit of the feedback capacitors, i.e., less than 150 photons, the detector is extremely fast and can handle more than 10^{12} photons/sec/pixel. Since the charge removal operation takes a certain amount of time, the sustainable flux is 10^8 photons/s/pixel, which is sufficient for the vast majority of the experiments at storage ring sources. However, this limitation makes the current MM-PAD

unsuitable for many FEL experiments, where more than 150 photons may arrive in a single pixel in a single pulse.

The Adaptive Gain Technique

A system of adapting the system's gain *during the integration phase* in response to the incoming photon signal was developed to meet the demand for XFEL-compatible detector systems that have extended dynamic range and single photon sensitivity for each pixel of each image at each time, independent of the image content. This concept (see Fig. 6) was pioneered by the PSI group with the GOTTHARD microstrip detector (Mozzanica et al. 2011, 2012) and has since been extended to multiple projects like the AGIPD and JUNGFRAU systems.

The basic idea is to use different feedback capacitors of successively larger sizes, three in the case of GOTTHARD and AGIPD, and to arrange the circuitry such that switching occurs automatically once a certain threshold voltage at the amplifier output is crossed. Switching points and feedback capacitor sizes have to be carefully matched in order to keep the system noise well below the Poisson limit for all x-ray possible signals. While the implementation of additional capacitors which are automatically switched in is relatively straightforward (see Fig. 6), data taking requires storing and reading the actual gain setting used in addition to the analog signal, which constitutes the presence of a second data path to the readout, much like that seen for the charge pump systems.

Utilizing Nonlinear Gain

An alternative to the stepwise adaptation of the gain, where the gain is real-time switched between different settings, each one being linear within its range, is to use a smoothly changing nonlinear gain. Ideally, the gain should have a square root dependence on the incoming signal strength. This would allow designs such that the noise is dominated by photon-counting statistics and not by the detector noise

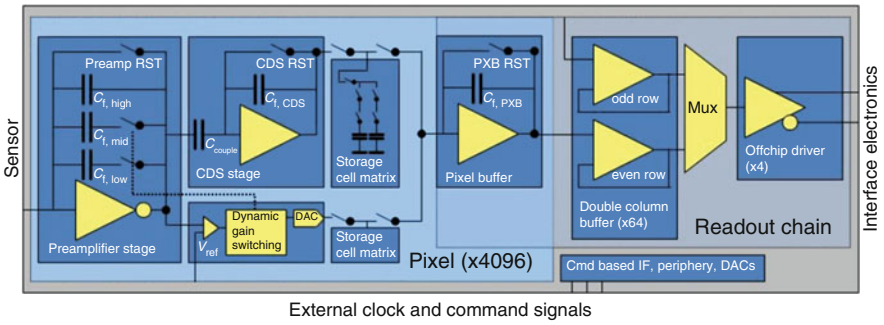

Fig. 6 Schematic block diagram of the most important ASIC components of AGIPD. The preamplifier stage features a threefold switching mechanism, which allows to adaptively change the gain in response to the input signal. The correlated double sampling (*CDS*) stage removes low-frequency noise from the system and the storage cell matrix is sufficient to store 352 separate images on the chip (Reproduced from Becker et al. 2013a)

over the entire operational range and at the same time provide the largest possible dynamic range for the available signal span.

One can implement nonlinear gains in the readout electronics. An approach to achieve nonlinearity by continuously changing the operating points of input transistors is shown in Fig. 7 (Fiorini et al. 2014). Another approach, using MOS capacitors as feedback capacitors in a classical integrator circuit, has already been demonstrated by the same group.

A different nonlinear gain approach is implemented by the DEPFET Sensor with Signal Compression (DSSC) project for the Eu-XFEL (Fischer et al. 2010; Lutz et al. 2010). DEPFETs allow for amplification on the sensor, and here, the nonlinearity is achieved by a special design of the internal gate of the DEPFET; see Fig. 8.

When only a few electrons are generated (weak signal), they are stored directly underneath the gate, hence giving the strongest effect on the source-drain current, thus a large gain. The more electrons are generated, the more they are stored away from the gate, thus having a reduced effect on the source-drain current, resulting in a reduced gain. This so-called signal compression in the sensor allows for simple

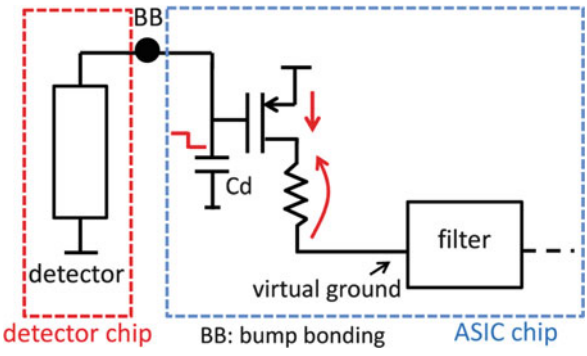

Fig. 7 Controlled nonlinearity introduced in the ASIC (Reproduced from Fiorini et al. 2014)

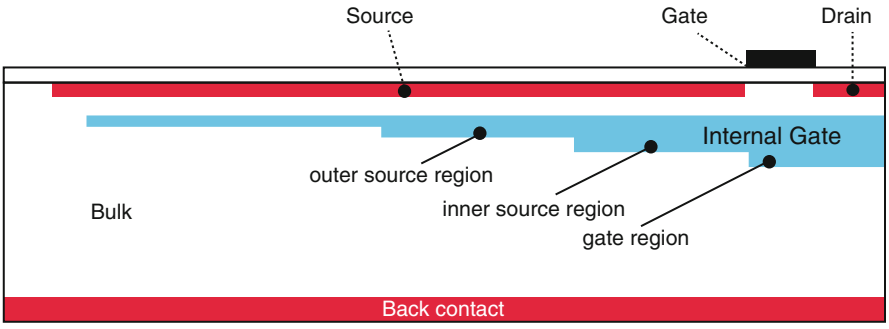

Fig. 8 Nonlinear gain of the DSSC sensor. The first signal electrons are collected in the potential well exactly below the gate. If that area is filled up with electrons, the next disk – extending below the source and the gate – collects electrons and so forth. Only the fraction of the additional charge that arrives below the internal gate is effective in modulating the transistor current (Reproduced from Porro et al. 2010)

readout electronics. Conversely, the production of such a nonlinear DEPFET sensor is by far nontrivial and can only be done by highly specialized laboratories.

Note that systems that rely on nonlinear schemes will require exceptionally careful calibrations to compensate for component variations inherent in integrated circuit processes and changes in circuit component properties over time and with accumulated radiation dose.

Frame Storage for High-Frequency Imaging

The extreme requirements of (multi) megahertz imaging at current and upcoming x-ray sources will demand measures beyond simple scaling in order to operate at these speeds. Even assuming that the first stages of the circuitry can be sped up sufficiently,[4] transmitting the resulting large volumes of data out of the detector plane is currently unfeasible.[5]

On-chip data processing and compression (e.g., zero suppression), a technique commonly employed by the high-energy physics community (Kästli et al. 2006), is of limited use in photon science, as image properties would have to be known beforehand, which they usually are not. In addition, the compression ratios of analog signals are low compared to those of photon counting systems. Thus, in order to frame at MHz rates, an in-circuit frame storage approach is commonly taken; this is sometimes also referred to as "burst mode" operation. A limited number of frames are stored locally at the desired frame rate and read out and transmitted off-chip at a later time, i.e., in between bursts. This off-chip transfer can happen at a lower speed than the frame rate. In this way, the frame rate and the data transfer rate become disentangled, allowing imaging at the desired speed.

While many different implementations of this idea exist and have been put into existence previously (e.g., frame store CCDs were developed in the early 1970s), most prominent current day implementations use either analog or digital storage cells inside the ASIC.

Digital Frame Store Method

Digital storage cells are essentially a nonvolatile digital memory included within the pixel circuitry in sufficient quantity to store the desired number of frames. The idea of using digital memory is very appealing as its circuit layout is commonly available as a highly optimized, small area standard cell for the selected process node, thus

[4]Charge collection in planar diode sensors of usual thickness typically requires 10–20 ns. Assuming 100 ns for ASIC pixel processing times, framing speeds of ∼10 MHz are feasible.

[5]Assuming a typical pixel size of 0.1×0.1 mm^2, 16 bit/sample and 1 million samples/s results in a data density of ∼1.5 Gbit/s/mm^2. For comparison, a typical SFP+ transceiver for 10 Gbit Ethernet is 8.5×13.4 mm^2, thereby transmitting less than 0.01 Gbit/s/mm^2, or a factor more than 150 less per same area.

saving valuable real estate in the pixel. It also minimizes layout and debugging time during design and production.

However, digital storage implies that the full analog processing chain, including the digitization, has to be completed at the frame rate. This translates to the requirement of fast in-pixel ADCs, which in turn require significant pixel area and power resources in order to operate at the desired high speeds and accuracies. Another disadvantage of this scheme is the fact that sensitive operations in the analog circuitry like the charge integration happens at the same time as the digitization, which is a potential source of cross talk.[6]

Analog Frame Store Method

Analog storage cells typically involve an array of sample-and-hold capacitors (e.g., Fig. 2) that decouple the speed of the first part of the readout chain (analog integration) from the speed of the last part (digitization and readout). In this way, one can ensure digital "silence" during the most sensitive part of analog operation, the charge integration, thereby reducing digital noise cross talk.

This potentially reduced noise comes at the price of a significant pixel area being devoted to storage capacitors. In addition, analog storage cells have to be designed to prevent leakage to/from adjacent silicon elements and through the CMOS addressing switches. Leakage increases with accumulated radiation dose making radiation-hardened integrated circuit layout methods important. All this takes even more pixel area. The consequences are shown in Fig. 9, showing the huge area taken by the analog storage memory in the AGIPD pixel. Leakage also increases with temperature, making low temperature operation advisable in certain cases.

Radiation Hardness

While much of an x-ray detector can be shielded from radiation, in an HPAD, the sensor and bonded ASICs are directly exposed to x-rays and, thus, are difficult to shield. The silicon bulk material is usually not damaged directly as the damage threshold for this is above a few 100 keV photon energy (Akkerman et al. 2001), but interfaces and oxide layers are susceptible to damage (Zhang et al. 2012a).

As the detectors discussed here are commonly exposed to immense radiation doses, measures are employed to ensure their functionality after high doses. In a radiation-tolerant detector design, radiation damage is manifest as gradual deterioration of detector performance with accumulated dose. Radiation damage is readily observed by users as increased dark current of the sensor – resulting in a shift of the signal offset in absence of photons – and an increased noise compared to undosed systems. Due to the increased intrinsic radiation hardness of the employed

[6]To avoid this, one can alternate digital and analog operations, but this reduces the maximum frame rate by a factor of 2.

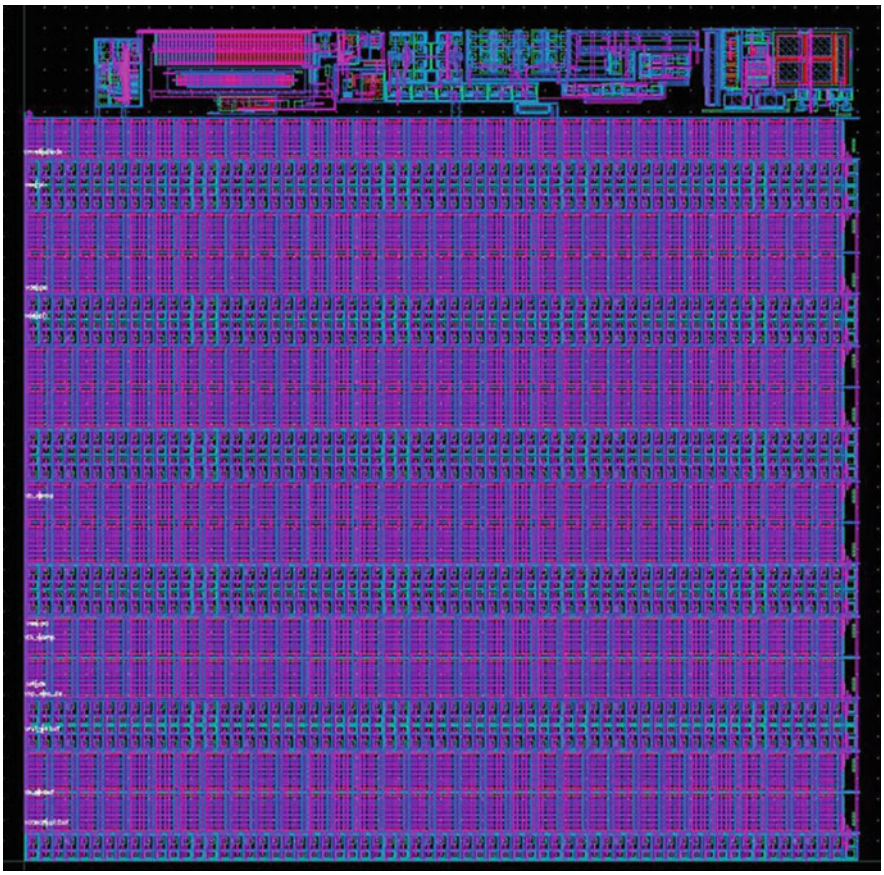

Fig. 9 Layout of the $(200\,\mu m)^2$ AGIPD pixel. The signal processing electronics only occupies the top part of the area (12.5 %); the rest is taken up by the 352 analog storage cells

submicron processes in modern detector ASICs, it is now relatively rare for chips to suddenly die from radiation-induced failure of the digital logic.

Some types of radiation-induced damage can be mitigated by thermal annealing. This is sometimes observed as a "recovery" with time of a heavily dosed part of a detector. Annealing of radiation-induced defects can be sped up by a high-temperature cycle; however, full annealing may require temperatures that are destructive to the detector system itself. Thus, there is a limit to the "self-healing" of heavily dosed detectors.

Radiation Damage to Sensors

Most HPAD sensors do not lose the basic ability to detect photons due to radiation per se, but rather exhibit increased noise, dark current and/or a reduction of the charge collection efficiency. Silicon sensors suffer mainly from charge buildup in

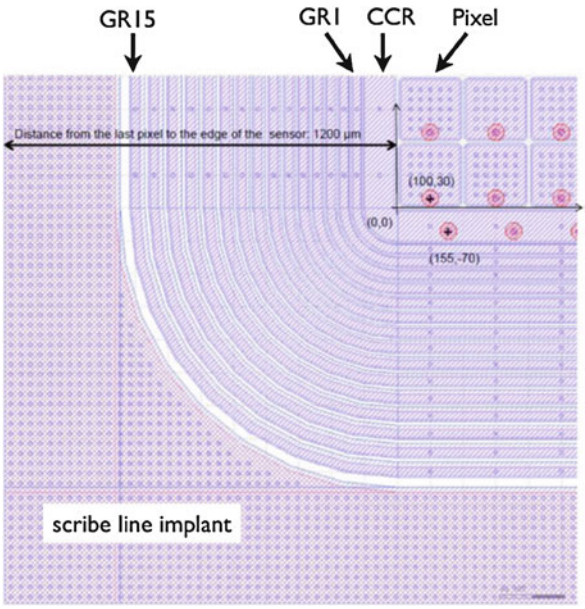

Fig. 10 Overview of the guard ring layout of the AGIPD sensor. Since AGIPD requires a voltage of 500 V or more to be applied, a special design of multiple guard rings is required to allow the use of high voltages after heavy dosing (Reproduced from Schwandt et al. 2013)

SiO_2 layers and generation of traps at the Si–SiO_2 interface. The mechanisms and effects of this are complex in detail (Schwandt 2014; Zhang et al. 2012b, a) and affect important operating parameters like the pixel capacitance and the breakdown voltage of the sensor. Without going into detail at this point, it is commonly accepted that the effects can partially be compensated for, but not completely avoided, by a dedicated layout of the sensor, especially by adequate guard rings that allow operation at higher bias voltages. An example of such a design is shown in the Fig. 10.

Similar mechanisms are found in other semiconductors used as sensors; however, each material has its individual response to high radiation dosage, e.g., "polarization" is a significant issue in CdTe sensors (Bell et al. 1974). In general, sensors operated as photoconductors are less affected than those operated as photodiodes.

Future Directions

Demand for specialized detection systems has risen with the establishment of more and brighter synchrotron and XFEL sources around the globe, and recent progress in solid-state x-ray detectors has been a consequence both of more people working in the field and advances in semiconductor and interconnect technologies. The continued increase of accessibility to circuit fabrication using submicron and deep submicron process technology allowed the development of detector systems with unprecedented characteristics. This trend is very likely to continue as more and more advanced capabilities become available at reasonable prices for small- and medium-scale developments. As the options of those advanced technologies can

appear limitless, a comprehensive listing is beyond the scope of this chapter and most probably would be outdated by the time of printing; hence, only two selected developments are mentioned here. Naturally, this section is biased and, since the future is uncertain by definition, the presented examples might be superseded by other developments.

3D-ASICS

In the drive for increased speed and higher integration densities, industry has developed technology whereby integrated circuits are connected together by so-called through-silicon vias, in addition to or replacing wire-bonding and printed circuit boards. Stacking of eight layers has been successfully demonstrated by a manufacturer of memory chips (Patti 2014), making this technique an attractive candidate for future detector applications. The principle of this 3D-ASIC technology is given in Fig. 11, showing the principle of face-to-face wafer bonding.

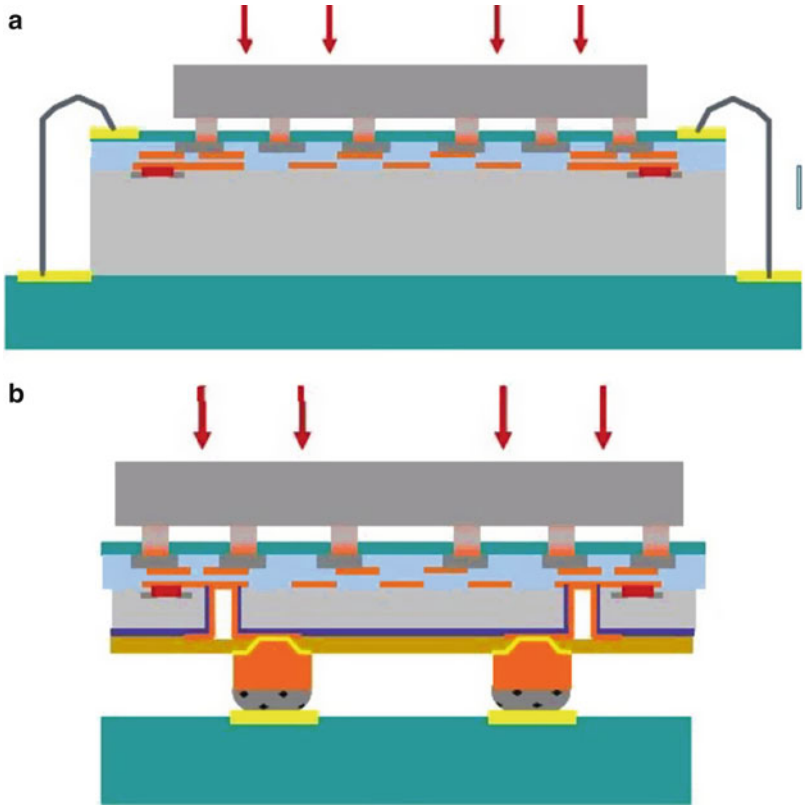

Fig. 11 (**a**) Current assembly of sensor to readout circuit. (**b**) New assembly of device connected by the solder ball grid array on the back side of the readout circuit chips using through-silicon vias (Reproduced from Henry et al. 2013)

The immediate advantage for HPADs is the increased functionality per unit area by putting additional processing capabilities in the second tier. This will allow for smaller pixels and/or smarter pixels. Prototype 2-tier ASICs have been developed by the 3D-AGIPD (Marras 2014) and the VIPIC (Deptuch et al. 2013) projects, respectively. As this technology matures, one may expect larger-scale deployment for scientific detector applications.

Ultrahigh Bandwidth Optical Transmission

The trend toward more (smaller) pixels and increased frame rates implies increased requirements in terms of data bandwidth. To illustrate this, one may look at the three systems developed for the Eu-XFEL. Each system will produce image data at rates of several gigabytes per second, which lead to the establishment of a dedicated data and computing center at Eu-XFEL.

Addressing the high-data rate challenge will require cooperation of experimentalists, beamline scientists, and research facilities alike as IT resources are likely to require significant upgrades.

At present, the bottleneck is the rate at which frames can be downloaded from detectors. However, laboratory tabletop experiments have demonstrated over 30 Tera-Bits/sec transmission speeds over a single optical fiber (Hillerkuss et al. 2010). Chip-level implementation of this technology is being developed and integrated into particle detectors within the Helmholtz Detector Technology and Systems Program (Helmholtz 2014). With these kinds of transmission speeds, raw data can quickly be transferred away from the detector to back-end processing farms. This has two distinct advantages: Firstly, it allows the front-end system to focus fully on its core activities, like amplification and digitization, freeing up resources otherwise dedicated to bandwidth reduction, e.g., on-chip processing and compression, resulting in optimized speed, reduced power consumption, small pixel sizes, and reduced overall form factor of the front-end detector. Secondly, the subsequent signal and data processing is performed on raw data away from the experiment, which allows for changes in certain parameters, e.g., thresholds, after-the-fact, thus maximizing the scientific usefulness of the acquired data, all while using commercially available, and thus rapidly evolving systems.

Summary

In the past, x-ray detector developments were often limited by the need to use components developed for other applications (e.g., CCDs) and materials issues (e.g., development of new phosphors or fiber optics). The ability to develop specialized ASICs and the availability of nearly perfect silicon sensors have resulted in a rapid development of HPADs. The impact on x-ray photon science at synchrotrons and FELs has been enormous.

The variety of integrating HPADs presented in this chapter follows the rapid developments in the semiconductor industry, from the Cornell 100 × 92 prototype realized in a 1.2 μm process, over the successfully used CS-PAD, MM-PAD, and Keck-PAD systems realized in 0.25 μm processes to the current-day prototypes like AGIPD, JUNGFRAU, and MÖNCH, realized in 130 and 110 nm technology. The move toward smaller feature sizes does not end here; projects using 65 and 40 nm processes, some in combination with 3D integration, have recently been started.

As this rapid evolvement of the semiconductor and electronics industry is likely to continue, so will the capabilities of HPADs, be they counting or integrating. HPADs will certainly overcome many of the constraints encountered today by utilizing advanced electronics and computing systems engineering. We may very well see different families of specialized HPADs designed for specific classes of experiments.

With the continued increase of capabilities, frequently paired with smaller pixel sizes, more pixels, and higher frame rates, the amount of scientific data per experiment will quickly increase beyond what is presently routinely seen and handled. While the total volume of the data streams is still within what can reasonably processed using state-of-the-art technology, it will be challenging to process the increased data volumes expected soon. As seen from current-day HPAD detectors, the actual sensor-ASIC hybridized chips that are the core detector elements are but a small part of the physical size of the overall size of a detector system. Much future development will occur in the remaining parts of the detector systems in order to handle data volume.

Finally, it is important to stress that over the last decade, it has indisputably been shown that the investments required to develop custom-designed detection systems have paid off. This has been true both for detectors used as stand-alone systems and detectors that have enabled scientific return of the large investments in large-scale synchrotron radiation facilities.

Acknowledgements SMG's x-ray detector development at Cornell University has been supported by the US Department of Energy, the National Science Foundation, and the Keck Foundation.

Cross-References

▸ Hybrid Pixel Photon Counting X-ray Detectors for Synchrotron Radiation

References

A. Akkerman, J. Barak, M. Chadwick, J. Levinson, M. Murat, Y. Lifshitz, Updated NIEL calculations for estimating the damage induced by particles and γ-rays in Si and GaAs. Radiat. Phys. Chem. **62**(4), 301–310 (2001)

K. Ayyer, H.T. Philipp, M.W. Tate, V. Elser, S.M. Gruner, Real-space x-ray tomographic reconstruction of randomly oriented objects with sparse data frames. Opt. Exp. **22**(3), 2403–2413 (2014)

R. Ballabriga, J. Alozy, G. Blaj, M. Campbell, M. Fiederle, E. Frojdh, E.H.M. Heijne, X. Llopart, M. Pichotka, S. Procz, L. Tlustos, W. Wong, The Medipix3RX: a high resolution, zero dead-time pixel detector readout chip allowing spectroscopic imaging. J. Instrum. **8**, C02016 (2013). doi:10.1088/1748-0221/8/02/C02016

S.L. Barna, J.A. Shepherd, R.L. Wixted, M.W. Tate, B. Rodricks, S.M. Gruner, Development of a fast pixel array detector for use in microsecond time-resolved x-ray diffraction. Proc. SPIE **2521**, 301–309 (1995)

J. Becker, L. Bianco, P. Gottlicher, H. Graafsma, H. Hirsemann, S. Jack, A. Klyuev, S. Lange, A. Marras, S. Rah, The high speed, high dynamic range camera AGIPD, in *IEEE Nuclear Science Symposium and Medical Imaging Conference (NSS/MIC)* (IEEE, 2013a). doi:10.1109/NSSMIC.2013.6829504

J. Becker, L. Bianco, P. Göttlicher, H. Graafsma, H. Hirsemann, S. Jack, A. Klyuev, S.L.A. Marras, U. Trunk, R. Klanner, Challenges for the adaptive gain integrating pixel detector (AGIPD) design due to the high intensity photon radiation environment at the European XFEL. (2013b). arXiv preprint arXiv:13032523

R. Bell, G. Entine, H. Serreze, Time-dependent polarization of CdTe gamma-ray detectors. Nucl. Instrum. Methods **117**(1), 267–271 (1974)

S. Boutet, L. Lomb, G.J. Williams, T.R.M. Barends, A. Aquila, R.B. Doak, U. Weierstall, D.P. DePonte, J. Steinbrener, R.L. Shoeman, M. Messerschmidt, A. Barty, T.A. White, S. Kassemeyer, R.A. Kirian, M.M. Seibert, P.A. Montanez, C. Kenney, R. Herbst, P. Hart, J. Pines, G. Haller, S.M. Gruner, H.T. Philipp, M.W. Tate, M. Hromalik, L.J. Koerner, N. van Bakel, J. Morse, W. Ghonsalves, D. Arnlund, M.J. Bogan, C. Caleman, R. Fromme, C.Y. Hampton, M.S. Hunter, L.C. Johansson, G. Katona, C. Kupitz, M. Liang, A.V. Martin, K. Nass, L. Redecke, F. Stellato, N. Timneanu, D. Wang, N.A. Zatsepin, D. Schafer, J. Defever, R. Neutze, P. Fromme, J.C.H. Spence, H.N. Chapman, I. Schlichting, High-resolution protein structure determination by serial femtosecond crystallography. Science **337**(6092), 362–364 (2012). doi:10.1126/science.1217737

W.Y. Cai, C.F. Powell, Y. Yue, S. Narayanan, J. Wang, M.W. Tate, M.J. Renzi, A. Ercan, E. Fontes, S.M. Gruner, Quantitative analysis of highly transient fuel sprays by time-resolved x-radiography. Appl. Phys. Lett. **83**(8), 1671–1673 (2003). doi:10.1063/1.1604161

G.W. Deptuch, G. Carini, T. Collier, P. Gryboś, P. Kmon, R. Lipton, P. Maj, M. Trimpl, D.P. Siddons, R. Szczygieł, Results of tests of three-dimensionally integrated chips bonded to sensors, in *Nuclear Science Symposium and Medical Imaging Conference (NSS/MIC), 2013*, Seoul, 27 Oct 2013 – 2 Nov 2013 (IEEE, 2013), pp. 1–5. doi:10.1109/NSSMIC.2013.6829434

R. Dinapoli, A. Bergamaschi, S. Cartier, D. Greiffenberg, I. Johnson, J. Jungmann, D. Mezza, A. Mozzanica, B. Schmitt, X. Shi, MÖNCH, a small pitch, integrating hybrid pixel detector for X-ray applications. J. Instrum. **9**(05), C05015 (2014)

A. Dragone, P. Caragiulo, B. Markovic, R. Herbst, B. Reese, S. Herrmann, P. Hart, J. Segal, G. Carini, C. Kenney, ePix: a class of architectures for second generation LCLS cameras. J. Phys.: Conf. Ser. **493**, 012012 (2014)

F. Erdinger, L. Bombelli, D. Comotti, S. Facchinetti, P. Fischer, K. Hansen, P. Kalavakuru, M. Kirchgessner, M. Manghisoni, M. Porro, The DSSC pixel readout ASIC with amplitude digitization and local storage for DEPFET sensor matrices at the European XFEL, in *IEEE Nuclear Science Symposium and Medical Imaging Conference (NSS/MIC)*, Anaheim (IEEE, 2012), pp. 591–596

C. Fiorini, B. Nasri, S. Facchinetti, L. Bombelli, P. Fischer, M. Porro, A simple technique for signal compression in high dynamic range, high speed X-ray pixel detectors. IEEE Trans. Nucl. Sci. (2014). doi:10.1109/tns.2014.2340899

P. Fischer, M. Bach, L. Bombelli, G. De Vita, F. Erdinger, S. Facchinetti, C. Fiorini, K. Hansen, S. Herrmann, P. Kalavakuru, Pixel readout ASIC with per pixel digitization and digital storage for the DSSC detector at XFEL, in *Nuclear Science Symposium Conference Record (NSS/MIC), 2010*, Knoxville (IEEE, 2010), pp. 336–341

K. Giewekemeyer, H.T. Philipp, R.N. Wilke, A. Aquila, M. Osterhoff, M.W. Tate, K.S. Shanks, A.V. Zozulya, T. Salditt, S. Gruner, High-dynamic-range coherent diffractive imaging:

ptychography using the mixed-mode pixel array detector. J. Synchrotron Radiat. **21**(5), 1167–1174 (2014)
D. Greiffenberg, The AGIPD detector for the European XFEL. J. Instrum. **7**(01), C01103 (2012)
S.M. Gruner, J.R. Milch, Criteria for the evaluation of 2-dimensional X-ray detectors. Trans. Am. Crystallogr. Assoc. **18**, 149–167 (1982)
S.M. Gruner, E. Eikenberry, M. Tate, Comparison of X-ray detectors, in International Tables for Crystallography, vol. F, ed. by M. Rossmann, E. Arnold (International Union of Crystallography, Kluwer Academic, London, 2001), pp. 143–147, 152-153
M. Hart, C. Angelsen, S. Burge, J. Coughlan, R. Halsall, A. Koch, M. Kuster, T. Nicholls, M. Prydderch, P. Seller, Development of the LPD, a high dynamic range pixel detector for the European XFEL, in *2012 IEEE Nuclear Science Symposium and Medical Imaging Conference (NSS/MIC)* (2012a), pp. 534–537. doi:10.1109/NSSMIC.2012.6551165
P. Hart, S. Boutet, G. Carini, M. Dubrovin, B. Duda, D. Fritz, G. Haller, R. Herbst, S. Herrmann, C. Kenney, The CSPAD megapixel x-ray camera at LCLS. Proc. SPIE **8504**, 85040C (2012b)
Helmholtz (2014) Helmholtz detector technology and systems program. See http://www.helmholtz-detectors.de/
B. Henrich, J. Becker, R. Dinapoli, P. Goettlicher, H. Graafsma, H. Hirsemann, R. Klanner, H. Krueger, R. Mazzocco, A. Mozzanica, The adaptive gain integrating pixel detector AGIPD a detector for the European XFEL. Nucl. Instrum. Methods Phys. Res. Sect. A: Accel. Spectrom. Detect. Assoc. Equip. **633**, S11–S14 (2011)
D. Henry, J. Alozy, A. Berthelot, R. Cuchet, C. Chantre, M. Campbell, TSV last for hybrid pixel detectors: application to particle physics and imaging experiments, in *2013 IEEE 63rd Electronic Components and Technology Conference (ECTC)* (IEEE, 2013), pp. 568–575. doi:10.1109/ECTC.2013.6575630
S. Herrmann, S. Boutet, B. Duda, D. Fritz, G. Haller, P. Hart, R. Herbst, C. Kenney, H. Lemke, M. Messerschmidt, CSPAD-140k: a versatile detector for LCLS experiments. Nucl. Instrum. Methods Phys. Res. Sect. A: Accel. Spectrom. Detect. Assoc. Equip. **718**, 550–553 (2013)
S. Herrmann, P. Hart, A. Dragone, D. Freytag, R. Herbst, J. Pines, M. Weaver, G. Carini, J. Thayer, O. Shawn, CSPAD upgrades and CSPAD V1.5 at LCLS. J. Phys.: Conf. Ser. **493**, 012013 (2014)
D. Hillerkuss, T. Schellinger, R. Schmogrow, M. Winter, T. Vallaitis, R. Bonk, A. Marculescu, J. Li, M. Dreschmann, J. Meyer, Single source optical OFDM transmitter and optical FFT receiver demonstrated at line rates of 5.4 and 10.8 Tbit/s, in *Optical Fiber Communication Conference* (Optical Society of America, 2010), p. PDPC1. doi:10.1364/OFC.2010.PDPC1
K.S. Im, S.K. Cheong, X. Liu, J. Wang, M.C. Lai, M.W. Tate, A. Ercan, M.J. Renzi, D.R. Schuette, S.M. Gruner, Interaction between supersonic disintegrating liquid jets and their shock waves. Phys. Rev. Lett. **102**(7), 074501 (2009). doi:10.1103/Physrevlett.102.074501
H.C. Kästli, M. Barbero, W. Erdmann, C. Hörmann, R. Horisberger, D. Kotlinski, B. Meier, Design and performance of the CMS pixel detector readout chip. Nucl. Instrum. Methods Phys. Res. Sect. A: Accel. Spectrom. Detect. Assoc. Equip. **565**(1), 188–194 (2006)
A. Koch, M. Kuster, J. Sztuk-Dambietz, M. Turcato, Detector development for the European XFEL: requirements and status. J. Phys.: Conf. Ser. **425**, 062013 (2013)
L.J. Koerner, S.M. Gruner, X-ray analog pixel array detector for single synchrotron bunch time-resolved imaging. J. Synchrotron Radiat. **18**, 157–164 (2011). doi:10.1107/s090904951004104x
L.J. Koerner, H.T. Philipp, M.S. Hromalik, M.W. Tate, S.M. Gruner, X-ray tests of a pixel array detector for coherent x-ray imaging at the linac coherent light source. J. Instrum. **4**, P03001 (2009a). doi:10.1088/1748-0221/4/03/P03001
L.J. Koerner, M.W. Tate, S.M. Gruner, An accumulating pixel array detector for single-bunch synchrotron experiments. IEEE Trans. Nucl. Sci. **56**(5), 2835–2842 (2009b). doi:10.1109/tns.2009.2028733
P.K. Lambert, C.J. Hustedt, K.S. Vecchio, E.L. Huskins, D.T. Casem, S.M. Gruner, M.W. Tate, H.T. Philipp, A.R. Woll, P. Purohit, J.T. Weiss, V. Kannan, K.T. Ramesh, P. Kenesei, J.S. Okasinski, J. Almer, M. Zhao, A.G. Ananiadis, T.C. Hufnagel, Time-resolved x-ray diffraction

techniques for bulk polycrystalline materials under dynamic loading. Rev. Sci. Instrum. **85**, 093901 (2014). doi:10.1063/1.4893881

X. Liu, J. Liu, X. Li, S.-K. Cheong, D. Shy, J. Wang, M.W. Tate, A. Ercan, D.R. Schuette, M.J. Renzi, A. Woll, S.M. Gruner, Development of ultrafast computed tomography of highly transient fuel sprays. Proc. SPIE **5535**, 21–28 (2004)

X. Liu, K.S. Im, Y. Wang, J. Wang, M.W. Tate, A. Ercan, D.R. Schuette, S.M. Gruner, Four dimensional visualization of highly transient fuel sprays by microsecond quantitative x-ray tomography. Appl. Phys. Lett. **94**(8), 084101 (2009)

W. Liu, D. Wacker, C. Gati, G.W. Han, D. James, D.J. Wang, G. Nelson, U. Weierstall, V. Katritch, A. Barty, N.A. Zatsepin, D.F. Li, M. Messerschmidt, S. Boutet, G.J. Williams, J.E. Koglin, M.M. Seibert, C. Wang, S.T.A. Shah, S. Basu, R. Fromme, C. Kupitz, K.N. Rendek, I. Grotjohann, P. Fromme, R.A. Kirian, K.R. Beyerlein, T.A. White, H.N. Chapman, M. Caffrey, J.C.H. Spence, R.C. Stevens, V. Cherezov, Serial femtosecond crystallography of G protein-coupled receptors. Science **342**(6165), 1521–1524 (2013)

G. Lutz, P. Lechner, M. Porro, L. Strüder, G. De Vita, DEPFET sensor with intrinsic signal compression developed for use at the XFEL free electron laser radiation source. Nucl. Instrum. Methods Phys. Res. Sect. A: Accel. Spectrom. Detect. Assoc. Equip. **624**(2), 528–532 (2010)

A.G. MacPhee, M.W. Tate, C.F. Powell, Y. Yue, M.J. Renzi, A. Ercan, S. Narayanan, E. Fontes, J. Walther, J. Schaller, S.M. Gruner, J. Wang, X-ray imaging of shock waves generated by high-pressure fuel sprays. Science **295**, 1261–1263 (2002). doi:10.1126/science.1068149

A. Marras, Towards a 3D-AGIPD. Presented in Front-End Electronics, 2014 (FEE2014), 19–23 May 2014. Argonne National Lab., USA (2014), https://indico.cern.ch/event/276611/session/7/contribution/25

MEDIPIX, http://knowledgetransfer.web.cern.ch/life-sciences/from-physics-to-medicine/medipix (2014)

A. Mozzanica, A. Bergamaschi, R. Dinapoli, H. Graafsma, B. Henrich, P. Kraft, I. Johnson, M. Lohmann, B. Schmitt, X. Shi, A single photon resolution integrating chip for microstrip detectors. Nucl. Instrum. Methods Phys. Res. Sect. A: Accel. Spectrom. Detect. Assoc. Equip. **633**, S29–S32 (2011)

A. Mozzanica, A. Bergamaschi, R. Dinapoli, H. Graafsma, D. Greiffenberg, B. Henrich, I. Johnson, M. Lohmann, R. Valeria, B. Schmitt, The GOTTHARD charge integrating readout detector: design and characterization. J. Instrum. **7**(01), C01019 (2012)

A. Mozzanica, A. Bergamaschi, S. Cartier, R. Dinapoli, D. Greiffenberg, I. Johnson, J. Jungmann, D. Maliakal, D. Mezza, C. Ruder, Prototype characterization of the JUNGFRAU pixel detector for SwissFEL. J. Instrum. **9**(05), C05010 (2014)

R. Patti, 2.5D and 3D integrated circuit technology capabilities and industry readiness (2014), www.tezzaron.com/Fmedia/Tezzaron-Presentation-Pixel-090414-for-posting.pdf

H.T. Philipp, L.J. Koerner, M. Hromalik, M.W. Tate, S.M. Gruner, Pixel array detector for the capture of femtosecond duration x-ray images. Proc. SPIE: Ultrafast X-Ray Sources Detect. **6703**, 67030O–67038 (2007)

H.T. Philipp, L.J. Koerner, M.S. Hromalik, M.W. Tate, S.M. Gruner, Femtosecond radiation experiment detector for X-ray free-electron laser (XFEL) coherent X-ray imaging. IEEE Trans. Nucl. Sci. **57**(6), 3795–3799 (2010). doi:10.1109/tns.2010.2085445

H.T. Philipp, M. Hromalik, M. Tate, L. Koerner, S.M. Gruner, Pixel array detector for X-ray free electron laser experiments. Nucl. Instrum. Methods Phys. Res. Sect. A: Accel. Spectrom. Detect. Assoc. Equip. **649**(1), 67–69 (2011). doi:10.1016/j.nima.2010.11.189

T. Poikela, J. Plosila, T. Westerlund, M. Campbell, M. De Gaspari, X. Llopart, V. Gromov, R. Kluit, M. van Beuzekom, F. Zappon, Timepix3: a 65K channel hybrid pixel readout chip with simultaneous ToA/ToT and sparse readout. J. Instrum. **9**(05), C05013 (2014)

M. Porro, L. Andricek, L. Bombelli, G. De Vita, C. Fiorini, P. Fischer, K. Hansen, P. Lechner, G. Lutz, L. Strüder, Expected performance of the DEPFET sensor with signal compression: a large format X-ray imager with mega-frame readout capability for the European XFEL. Nucl. Instrum. Methods Phys. Res. Sect. A: Accel. Spectrom. Detect. Assoc. Equip. **624**(2), 509–519 (2010)

L. Redecke, K. Nass, D.P. DePonte, T.A. White, D. Rehders, A. Barty, F. Stellato, M.N. Liang, T.R.M. Barends, S. Boutet, G.J. Williams, M. Messerschmidt, M.M. Seibert, A. Aquila, D. Arnlund, S. Bajt, T. Barth, M.J. Bogan, C. Caleman, T.C. Chao, R.B. Doak, H. Fleckenstein, M. Frank, R. Fromme, L. Galli, I. Grotjohann, M.S. Hunter, L.C. Johansson, S. Kassemeyer, G. Katona, R.A. Kirian, R. Koopmann, C. Kupitz, L. Lomb, A.V. Martin, S. Mogk, R. Neutze, R.L. Shoeman, J. Steinbrener, N. Timneanu, D.J. Wang, U. Weierstall, N.A. Zatsepin, J.C. SpenceH, P. Fromme, I. Schlichting, M. Duszenko, C. Betzel, H.N. Chapman, Natively inhibited trypanosoma brucei cathepsin B structure determined by using an X-ray laser. Science **339**(6116), 227–230 (2013)

G. Rossi, M. Renzi, E.F. Eikenberry, M.W. Tate, D. Bilderback, E. Fontes, R. Wixted, S. Barna, S.M. Gruner, Tests of a prototype pixel array detector for microsecond time-resolved X-ray diffraction. J. Synchrotron Radiat. **6**, 1096–1105 (1999)

D.R. Schuette, A mixed analog and digital pixel array detector fro synchrotron x-ray imaging. Ph.D. thesis, Cornell University, Ithaca (2008)

J. Schwandt, Design of a radiation hard silicon pixel sensor for X-ray science. Ph.D. thesis, University of Hamburg, Hamburg (2014)

J. Schwandt, E. Fretwurst, R. Klanner, J. Zhang, Design of the AGIPD sensor for the European XFEL. J. Instrum. **8**(01), C01015 (2013)

S. Shapiro, Pixel detector workshop. Synchrotron Radiat. News **3**(3), 6–8 (1990)

X. Shi, R. Dinapoli, B. Henrich, A. Mozzanica, B. Schmitt, R. Mazzocco, H. Krüger, U. Trunk, H. Graafsma, Challenges in chip design for the AGIPD detector. Nucl. Instrum. Methods Phys. Res. Sect. A: Accel. Spectrom. Detect. Assoc. Equip. **624**(2), 387–391 (2010)

M.W. Tate, D. Chamberlain, K.S. Green, H.T. Philipp, P. Purohit, C. Strohman, S.M. Gruner, A medium-format, mixed-mode pixel array detector for kilohertz x-ray imaging. J. Phys.: Conf. Ser. **425**, 062009 (2013)

J.C. Trenkle, L.J. Koerner, M.W. Tate, S.M. Gruner, T.P. Weihs, T.C. Hufnagel, Phase transformations during rapid heating of Al/Ni multilayer foils. Appl. Phys. Lett. **93**(8), 081903 (2008). doi:10.1063/1.2975830

J. Trenkle, L. Koerner, M. Tate, N. Walker, S. Gruner, T. Weihs, T. Hufnagel, Time-resolved x-ray microdiffraction studies of phase transformations during rapidly propagating reactions in Al/Ni and Zr/Ni multilayer foils. J. Appl. Phys. **107**(11), 113511 (2010)

W. Vernon, M. Allin, R. Hamlin, T. Hontz, D. Nguyen, F. Augustine, S.M. Gruner, N.H. Xuong, D.R. Schuette, M.W. Tate, L.J. Koerner, First results from the 128 × 128 pixel mixed-mode Si x-ray detector chip. Proc. SPIE **6706**, 67060U (2007). doi:10.1117/12.738663

J. Zhang, E. Fretwurst, R. Klanner, I. Pintilie, J. Schwandt, M. Turcato, Investigation of X-ray induced radiation damage at the Si-SiO2 interface of silicon sensors for the European XFEL. J. Instrum. **7**(12), C12012 (2012a)

J. Zhang, I. Pintilie, E. Fretwurst, R. Klanner, H. Perrey, J. Schwandt, Study of radiation damage induced by 12 keV X-rays in MOS structures built on high-resistivity n-type silicon. J. Synchrotron Radiat. **19**(3), 340–346 (2012b)